SEPARATION SCIENCE AND TECHNOLOGY
Vol. 39, No. 2, pp. 245–270, 2004

Design of SMB Chiral Separations Using the Concept of Separation Volume

Alírio E. Rodrigues[1,*] and Luís S. Pais[1,2]

[1]Laboratory of Separation and Reaction Engineering, School of Engineering, University of Porto, Porto, Portugal
[2]School of Technology and Management, Bragança Polytechnic Institute, Bragança, Portugal

ABSTRACT

The article deals with chiral separation by simulated moving bed (SMB) chromatography. When mass transfer resistances are negligible, equilibrium theory provides explicit criteria for the choice of the SMB operating conditions. However, in the presence of mass transfer resistances, the SMB operating conditions should be evaluated through simulation. Using a package based on the analogy with the true moving bed operation, this work shows how mass transfer resistance can affect the conditions for enantiomers separation, as well as the critical values stated by equilibrium theory. The concept of separation volume is applied to show how the flow-rate constraints, in presence of mass transfer

*Correspondence: Alírio E. Rodrigues, Laboratory of Separation and Reaction Engineering, School of Engineering, University of Porto, Rua Dr. Roberto Frias s/n, 4200-465, Porto, Portugal; Fax: 351-22-508-1674; E-mail: arodrig@fe.up.pt.

DOI: 10.1081/SS-120027557 0149-6395 (Print); 1520-5754 (Online)

resistances, have to be modified for chiral separations in which the adsorption equilibrium isotherms of both enantiomers are of linear + Langmuir type.

Key Words: Separation volume; Simulated moving bed; Chiral separation; Modeling; Numerical simulation.

INTRODUCTION

For many years it was common practice to market chiral drugs as racemates. However, the situation is rapidly changing and, since the early nineties, there has been an increasing interest in the separation of racemic mixtures, especially for therapeutic purposes. When chiral drugs are made without including an enantiomeric reagent or catalyst in their synthesis, the result is a 50–50 mixture of the two enantiomers, called racemate. These two enantiomers frequently have different biological activity: one enantiomer can be beneficial; whereas the other may not have the same function. Instead, the second isomer may be inactive or, in the worst scenario, may have adverse properties. Consequently, regulatory agencies require now the drug developers to quantify the pharmacological and toxicological effects of individual enantiomers as well as the racemate, and to produce a single enantiomer drug substance if the result of either the pharmacokinetics or the toxicological of the enantiomers is significantly different.[1,2]

Basically, there are two approaches to obtain enantiomerically pure compounds. The first consists of preparing the racemic material that is later resolved into its two enantiomeric forms. The second method is based on a stereoselective synthesis and leads to the production of only one enantiomer. This last approach has been widely used although, in many cases, the process can be uneconomical due to the greater number of steps and the costly enantiomeric reagents needed.[3] Moreover, the yields of these processes are often low or moderate at best.[2]

Chiral chromatographic resolution of enantiomeric species is becoming of increasing importance in the development and the production of pharmaceutical drugs. In the past, large-scale chromatographic separations were limited, mainly due to the high cost of the adsorbent, the high dilution of products, and the large amounts of mobile phase needed. In view of these demands, simulated moving bed (SMB) technology[4] has been recently applied to the pharmaceutical industry. Its use on a production scale has been considered as an alternative to the up to now leading techniques, such as enantioselective synthesis or diastereoisomeric crystallization. Several pharmaceutical companies and custom chemical manufacturers are installing

MARCEL DEKKER, INC.
270 Madison Avenue, New York, New York 10016

commercial-scale SMB units for producing enantiomeric compounds. The list is rapidly increasing and includes Aerojet Fine Chemicals (USA), Bayer (Germany), CarboGen Laboratories (Switzerland), Chiral Technologies (USA), Daicel (Japan), Honeywell Specialty Chemicals (Ireland), H. Lundbeck (Denmark), Merck (Germany), UCB Pharma (Belgium), and Universal Pharma Technologies (USA).[5–9]

A SMB adsorber is essentially a binary separator, so it is particularly appropriate for chiral separations. Briefly, SMB chromatography allows the continuous injection and separation of binary mixtures. The simulated countercurrent contact between the solid and liquid phases maximizes the mass-transfer driving force, leading to a significant reduction in mobile and stationary phases consumption when compared with conventional batch chromatography. Hence, with SMB technology, large-scale separations can now be carried out under cost-effective conditions.[10–13]

The principle of SMB operation can be best understood by reference to the equivalent true moving bed (TMB) process. In the ideal TMB operation, liquid and solid flow in opposite directions (Fig. 1). Furthermore, liquid and adsorbent streams are continuously recycled: the liquid flowing out of Section 4 is recycled to Section 1, while the solid coming out of Section 1 is recycled to Section 4. The feed is continuously injected in the middle of the system and two product lines can be collected: the extract, rich in the compounds that are more retained and so preferentially carried with the solid phase, and the raffinate, rich in the less retained species that move upward with the liquid phase. Pure eluent is continuously injected at the beginning of Section 1, with the liquid recycled from the end of Section 4. In the TMB operation, the solid flow rate is constant all over the unit. However, due to the injection and withdrawal points, the liquid flow rates differ from section to section, allowing the four sections of the unit to perform different functions.

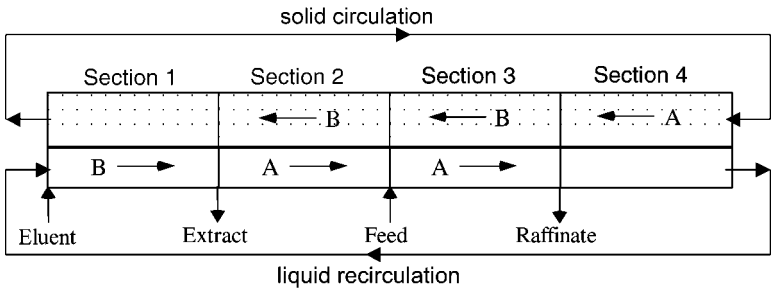

Figure 1. Schematic diagram of a TMB with the desired net fluxes of the two components in each section.

Marcel Dekker, Inc.
270 Madison Avenue, New York, New York 10016

The operation of a TMB introduces problems concerning the movement of the solid phase. A uniform flow of both solid and liquid is difficult to obtain. Also, mechanical erosion of the adsorbent phase will occur. In view of these difficulties, a SMB technique was developed to retain the process advantages of continuous and countercurrent flow without introducing the problems associated with the actual movement of the solid phase.[4,14] In the SMB system, the solid phase is fixed and the positions of the inlet and outlet streams move periodically. This shift, carried out in the same direction of the liquid phase, simulates the movement of the solid phase in the opposite direction. However, it is impractical to move the liquid inlet and withdrawal positions continuously. Nevertheless, approximately the same effect can be obtained by dividing the adsorbent bed into a number of fixed-bed columns and providing multiple access lines for the liquid streams between each column. Thereby, the four liquid access lines between each column can be used to perform a discrete movement of the inlet and outlet streams in the same direction of the liquid phase.

The selection of the SMB operating conditions is not straightforward. The main problem of the SMB operation consists in choosing the right solid (switch time interval) and liquid flow rates. Designed for high-productivity separations, SMB units usually operate at high-feed concentrations, leading to nonlinear competitive adsorption behaviors. Therefore, modeling and simulation tools are of crucial importance before running the system. The problem of modeling a SMB separation process can be analyzed by two different strategies: one, by simulating the system directly, taking into account its intermittent behavior, the other by representing its operation in terms of a true countercurrent system. The first model represents the real SMB and considers the periodic switch of the injection and collection points. The second is developed by assuming the equivalence with the true moving bed, where solid and fluid phases flow in opposite directions. Several academic contributions in this field were published in the last years and a literature survey on the subject can be found elsewhere.[5,6,15–17]

The model used in this work considers axial dispersion flow for the bulk fluid phase, and the linear driving force (LDF) approximation is used to describe the intraparticle mass transfer rate. This and more complex models, such as the inclusion of a bilinear driving force approximation to account for intraparticle diffusion or the assumption of noninstantaneous equilibrium at the solid–fluid interface, were used by our group to study the effects of deviations from the equilibrium, particularly the effects of mass transfer resistances on the performance of SMB units.[18–25]

The objective of this work was to study the influence of mass transfer resistance on the selection of the SMB operating conditions and on the flow-rate constraints for nonlinear chromatographic separations of enantiomers.

MARCEL DEKKER, INC.
270 Madison Avenue, New York, New York 10016

In particular, the concept of separation volume was used to illustrate how the flow-rate constraints have to be modified in presence of mass transfer resistances and how these modifications affect the performance of the SMB process in terms of solvent consumption and adsorbent productivity.

DESIGN OF SMB CHIRAL SEPARATIONS

The prediction of the SMB operation can be carried out through the equivalent TMB approach, if the SMB system has a certain degree of subdivision of the adsorbent bed. As it was shown in a previous work,[17] for SMB units with, at least, two columns per section, the steady-state performance as well as the concentration internal profiles can be properly evaluated by using the TMB model. For the particular chiral system studied in this work and described later, and for the operating conditions and model parameters presented later in Table 4, numerical simulations using both SMB and TMB models show very similar results in terms of extract and raffinate purities. For a mass-transfer coefficient of $k = 0.22\,s^{-1}$, the TMB model predicts 100% pure extract and raffinate, while the SMB model predicts 99.9% for extract and 100% for raffinate. For $k = 0.165\,s^{-1}$, TMB predicts 99.9 and 100%, counter the prediction for SMB, 99.6 and 99.9%. For $k = 0.11\,s^{-1}$, TMB predicts 99.3 and 99.6%, counter the prediction for SMB, 98.4 and 99.1%. Note that $k = 0.11\,s^{-1}$ is the lower value of the mass-transfer coefficient used in this work. On the other hand, the objective of this work was to study the influence of mass transfer resistances on the SMB performance, and compare it to the one predicted by the equilibrium theory. Since equilibrium theory also uses the true moving bed equivalence, the TMB model was used to ensure an effective comparison.

The design problem of a TMB consists of setting the flow rates in each section to obtain the desired separation. Some constraints have to be met if one wants to recover the less adsorbed component A in the raffinate and the more retained component B in the extract. These constraints are expressed in terms of the net fluxes of components in each section. As it was pointed out earlier (see Fig. 1), in Section 1, both species must move upward, in Sections 2 and 3, the light species must move upward, while the net flux of the more retained component must be downward, and in Section 4, the net flux of both species have to be downward, i.e.,

$$\begin{aligned} &\frac{Q_1 c_{B1}}{Q_S q_{B1}} > 1;\ \frac{Q_2 c_{A2}}{Q_S q_{A2}} > 1 \quad \text{and} \quad \frac{Q_2 c_{B2}}{Q_S q_{B2}} < 1 \\ &\frac{Q_3 c_{A3}}{Q_S q_{A3}} > 1 \quad \text{and} \quad \frac{Q_3 c_{B3}}{Q_S q_{B3}} < 1;\ \frac{Q_4 c_{A4}}{Q_S q_{A4}} < 1 \end{aligned} \tag{1}$$

Marcel Dekker, Inc.
270 Madison Avenue, New York, New York 10016

where Q_1, Q_2, Q_3, and Q_4 are the volumetric liquid flow rates in the various sections of the TMB, Q_S is the solid flow rate, c_{Aj} and c_{Bj} are the concentrations of species A and B in the liquid phase, and q_{Aj}, q_{Bj} are the adsorbed concentrations of components A and B, in section j. The same constraints can be expressed alternatively in terms of fluid and solid interstitial velocities. Defining the dimensionless parameter $\gamma_j = v_j/u_s$ as the ratio between fluid and solid interstitial velocities in zone j and $\varepsilon/(1-\varepsilon)$ as the ratio between fluid and solid volumes, the constraints defined by Eq. (1) become:

$$\begin{aligned} &\gamma_1 > \frac{1-\varepsilon}{\varepsilon}\frac{q_{B1}}{c_{B1}} \quad \frac{1-\varepsilon}{\varepsilon}\frac{q_{A2}}{c_{A2}} < \gamma_2 < \frac{1-\varepsilon}{\varepsilon}\frac{q_{B2}}{c_{B2}} \\ &\frac{1-\varepsilon}{\varepsilon}\frac{q_{A3}}{c_{A3}} < \gamma_3 < \frac{1-\varepsilon}{\varepsilon}\frac{q_{B3}}{c_{B3}} \qquad \gamma_4 < \frac{1-\varepsilon}{\varepsilon}\frac{q_{A4}}{c_{A4}} \end{aligned} \tag{2}$$

For the case of a binary system with linear adsorption isotherms, $q_{ij}/c_{ij} = K_i$ is constant, and very simple formulas can be derived to evaluate the better TMB flow-rates.[15] For nonlinear systems, however, the evaluation of the better flow rates is not straightforward. It is well known that, for the majority of the binary systems (chiral mixtures included), the adsorption behavior must be described with more complex models, such as, the nonlinear competitive adsorption isotherm. For this kind of system, the adsorbed concentration of a component in equilibrium with its concentration in the liquid phase depends not only on its own, but also on all other species, concentrations. It means that the ratio between the adsorbed-phase and fluid-phase concentrations that influences the net fluxes of both components in the TMB operation [Eqs. (1) or (2)] is no longer constant but concentration-dependent.

Morbidelli and co-workers developed a complete design of the binary countercurrent separation processes by SMB chromatography in the frame of the equilibrium theory. They assumed that mass transfer resistances and axial dispersion are negligible, and the adsorption equilibria were described through a variable selectivity modified Langmuir isotherm.[26] The conditions to achieve complete separation were evaluated considering the equivalent true moving bed operation. Following the assumptions of the equilibrium theory, they provided explicit criteria for the choice of the SMB operating conditions that lead to complete separation of a binary mixture. The region for complete separation was defined in terms of the flow-rate ratios in the four sections of the equivalent true moving bed unit, m_j, and are related to the γ_j ratios used in this work by $\gamma_j = (1-\varepsilon)m_j/\varepsilon$.

MARCEL DEKKER, INC.
270 Madison Avenue, New York, New York 10016

Table 1 presents the necessary and sufficient conditions for complete separation considering Langmuir isotherms:

$$q_i^* = \frac{Qb_iC_i}{1 + b_AC_A + b_BC_B}, \quad (i = A, B) \tag{3}$$

The equations presented in Table 1 can also be used when a modified Langmuir isotherm (linear + Langmuir) is considered:

$$q_i^* = mC_i + \frac{Qb_iC_i}{1 + b_AC_A + b_BC_B}, \quad (i = A, B) \tag{4}$$

In this case, the complete separation region provided by the equations presented in Table 1 must be shifted by using the relation $m_j^L = m_j^L + m$, where m_j^L is the value obtained considering only the Langmuir term (by using equations in Table 1) and m is the linear coefficient of the linear + Langmuir isotherm [Eq. (4)].

However, several investigators have noticed that deviations from the equilibrium due to nonideal effects, such as axial dispersion and mass transfer resistances, have important influences on the purity performance of the SMB process. This is true for linear systems[22–24,27–30] and also for systems described by nonlinear adsorption behaviors.[18–20,31–37] Consequently, if mass transfer effects are important, the operating conditions obtained by the equilibrium theory design must be modified, i.e., the region for complete separation defined by the equilibrium approach is reduced under nonideal conditions.[18,19,22,23,35,36] As we will show in the present work, mass transfer resistance can modify the better SMB operating conditions, leading to significant differences in the performance parameters such as productivity and solvent consumption. As it was already noticed for linear systems,[22] the constraints for Sections 1 and 4 will also be changed and will no longer depend solely on equilibrium data. The simulation studies show that there are new limiting values for the flow-rate constraints in the presence of mass transfer effects. This is better illustrated by using the concept of separation volume, which allows visualization in a three-dimensional (3-D) plot, e.g., $\gamma_1 \times \gamma_2 \times \gamma_3$ of the volume region where separation can be achieved within the purity constraints fixed by the operator.

Steady-State TMB Model

To predict the steady-state performance of a SMB separation process, one can use the TMB model with obvious advantages in computing timesavings.

MARCEL DEKKER, INC.
270 Madison Avenue, New York, New York 10016

Table 1. Operating conditions for complete separation under equilibrium theory: Langmuir adsorption isotherms.[26]

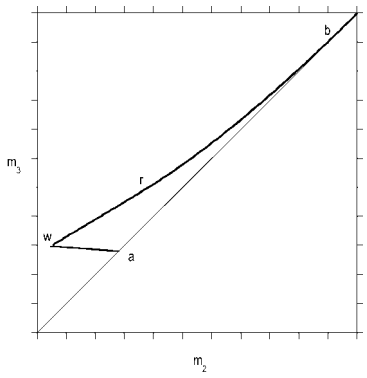

$$\lambda_B = m_{1,\min} < m_1 < \infty \tag{5}$$

$$m_{2,\min}(m_2, m_3) < m_2 < m_3 < m_{3,\max}(m_2, m_3) \tag{6}$$

$$0 < m_4 < m_{4,\max}(m_2, m_3) = \frac{1}{2}\left\{\lambda_A + m_3 + b_A {C_A}^F (m_3 - m_2) - \sqrt{[\lambda_A + m_3 + b_A {C_A}^F (m_3 - m_2)]^2 - 4\lambda_A m_3}\right\} \tag{7}$$

Boundaries of the complete separation region in the (m_2, m_3) plane:

Straight line wr: $[\lambda_B - \omega_G\,(1 + b_B\,C_B^F)]\,m_2 + b_B\,C_B^F\,\omega_G\,m_3 = \omega_G\,(\lambda_B - \omega_G)$;
Straight line wa: $[\lambda_B - \lambda_A\,(1 + b_B\,C_B^F)]\,m_2 + b_B\,C_B^F\,\lambda_A\,m_3 = \lambda_A\,(\lambda_B - \lambda_A)$;
Curve rb: $m_3 = m_2 + \dfrac{(\sqrt{\lambda_B} - \sqrt{m_2})^2}{b_B {C_B}^F}$; Straight line ab: $m_3 = m_2$ (8)

The coordinates of the intersection points are given by:

point a: (λ_A, λ_A); point b: (λ_B, λ_B);

point r: $\left(\dfrac{{\omega_G}^2}{\lambda_B}, \dfrac{\omega_G[\omega_F(\lambda_B - \omega_G)(\lambda_B - \lambda_A) + \lambda_A\omega_G(\lambda_B - \omega_F)]}{\lambda_A\lambda_B(\lambda_B - \omega_F)}\right)$

and

point w: $\left(\dfrac{\lambda_A\omega_G}{\lambda_B}, \dfrac{\omega_G[\omega_F(\lambda_B - \lambda_A) + \lambda_A(\lambda_A - \omega_F)]}{\lambda_A(\lambda_B - \omega_F)}\right)$ (9)

(*continued*)

MARCEL DEKKER, INC.
270 Madison Avenue, New York, New York 10016

Table 1. Continued.

with $\omega_G > \omega_F > 0$, which are given by the roots of the following quadratic equation:

$$(1 + b_A C_A{}^F + b_B C_B{}^F)\omega^2 - [\lambda_A(1 + b_B C_B{}^F) + \lambda_B(1 + b_A C_A{}^F)]\omega + \lambda_A \lambda_B = 0 \tag{10}$$

In the above equations, C_A^F and C_B^F are the feed concentrations of species A and B, respectively, and $\lambda_i = Qb_i$, $(i = A, B)$.

Moreover, if we are interested in characterizing only the steady-state operation, we can develop a steady-state TMB model, which is simpler to implement. In fact, the original problem represented by a set of partial differential equations will be simplified to a set of ordinary differential equations.

The SMB performance under nonlinear conditions and considering mass transfer resistance was evaluated by numerical simulation. The model equations result from the mass balances over a volume element of the bed and at a particle level. Axial dispersion flow for the bulk fluid phase is included and the linear driving force approximation is used to describe the intraparticle mass transfer rate. Table 2 summarizes the steady-state TMB model equations, boundary conditions, and mass balances at the nodes between each section. The resulting model parameters are: the ratio between solid and fluid volumes, $(1 - \varepsilon)/\varepsilon$; the ratio between fluid and solid interstitial velocities, $\gamma_j = v_j/u_s$; the Peclet number, $Pe = v_j L_j / D_{Lj}$; the number of mass transfer units, $\alpha_j = kL_j/u_s$; and the adsorption equilibrium parameters.

The steady-state TMB model presented before was numerically solved by using *COLNEW* software.[38] This package solves a general class of mixed-order systems of boundary value ordinary differential equations and is a modification of the *COLSYS* package developed by Ascher et al.[39,40] Each section of the TMB unit is defined by four ordinary differential equations (ODEs): for each component, there is an ODE resulting from the mass balance in a volume element of the bed and another resulting from the mass balance in the particle. Since the TMB unit is composed by four sections, and considering a binary separation, the steady-state TMB model is defined by a set of 16 ODEs.

Performance Parameters

To characterize the steady-state SMB performance, three process parameters are used: purity, productivity, and solvent consumption. These parameters are defined for the case of a binary separation (racemic mixture) in

MARCEL DEKKER, INC.
270 Madison Avenue, New York, New York 10016

Table 2. Model equations for the steady-state TMB model.

Mass balance in a volume element of the bed j:

$$\frac{1}{Pe_j}\frac{d^2c_{ij}}{dx^2} - \frac{dc_{ij}}{dx} - \frac{1-\varepsilon}{\varepsilon}\frac{\alpha_j}{\gamma_j}(q^*_{ij} - q_{ij}) = 0 \tag{11}$$

Mass balance in the particle:

$$\frac{dq_{ij}}{dx} + \alpha_j(q^*_{ij} - q_{ij}) = 0 \tag{12}$$

Boundary conditions for section j:

$$x = 0: \qquad c_{ij} - \frac{1}{Pe_j}\frac{dc_{ij}}{dx} = c_{ij,0} \tag{13}$$

where $c_{ij,0}$ is the inlet concentration of species i in section j.

$$\begin{aligned} x = 1: \quad & \text{for the eluent node, } c_{i4} = \frac{v_1}{v_4}c_{i1,0}; \\ & \text{for the extract node, } c_{i1} = c_{i2,0}; \\ & \text{for the feed node, } c_{i2} = \frac{v_3}{v_2}c_{i3,0} - \frac{v_F}{v_2}c_i{}^F; \\ & \text{for the raffinate node, } c_{i3} = c_{i4,0} \end{aligned} \tag{14}$$

and

$$q_{i4} = q_{i1,0},\ q_{i1} = q_{i2,0},\ q_{i2} = q_{i3,0},\ q_{i3} = q_{i4,0} \tag{15}$$

Global balances:

$$\begin{aligned} & \text{eluent node, } v_1 = v_4 + v_E; \text{ extract node, } v_2 = v_1 - v_X; \\ & \text{feed node, } v_3 = v_2 + v_F; \text{ raffinate node, } v_4 = v_3 - v_R \end{aligned} \tag{16}$$

Multicomponent adsorption equilibrium isotherm:

$$q^*_{Aj} = f_A(c_{Aj}, c_{Bj}) \qquad \text{and} \qquad q^*_{Bj} = f_B(c_{Aj}, c_{Bj}) \tag{17}$$

Note: In the above equations, $i = A, B$ refers to the species in the mixture, and $j = 1, 2, 3, 4$ is the section number.

Marcel Dekker, Inc.
270 Madison Avenue, New York, New York 10016

which the less retained species A is recovered in the raffinate and the more retained component B is recovered in the extract. The purity is defined for both product lines, extract and raffinate. Extract purity is defined as the ratio between the concentration of the more retained component and the total concentration of the two species in the extract. An analogous definition is used for raffinate purity, considering that the target compound is now the less retained species. A productivity parameter is also defined for each component; it corresponds to the total amount of the target species produced in the correspondent outlet line (extract for B, raffinate for A) divided by the total volume of adsorbent used. Solvent consumption is defined as the total amount of solvent used (in eluent and feed) per unit of racemic amount treated. Table 3 summarizes the performance parameters used.

RESULTS AND DISCUSSION

Chiral System

The chromatographic resolution of a racemic mixture of chiral epoxide enantiomers (Sandoz Pharma, Basel, Switzerland) was considered for simulation purposes. The chiral stationary phase used in this system is microcrystalline cellulose triacetate (Merck, Darmstadt, Germany) with an average particle diameter of 45 μm and pure methanol used as eluent. The adsorption equilibrium isotherms were measured at 25°C and are represented by a linear + Langmuir competitive model:[19]

$$q_A^* = 1.35C_A + \frac{7.32 \times 0.087C_A}{1 + 0.087C_A + 0.163C_B} \tag{18a}$$

$$q_B^* = 1.35C_B + \frac{7.32 \times 0.163C_B}{1 + 0.087C_A + 0.163C_B} \tag{18b}$$

The chromatographic resolution of these chiral epoxide enantiomers was experimentally carried out using SMB technology (Licosep 12-26 pilot unit,

Table 3. SMB performance parameters.

Performance parameters	Extract	Raffinate
Purity (%)	$100C_B^X/(C_A^X + C_B^X)$	$100C_A^R/(C_A^R + C_B{}^R)$
Productivity (g/day L_{bed})	$Q_X C_B^X/V_{bed}$	$Q_R\, C_A^R/V_{bed}$
Solvent consumption (L/g)	$(Q_E + Q_F)/(Q_F(C_A^F + C_B^F))$	

Novasep, France) under operating conditions similar to the ones used in this work: eight chromatographic columns ($D_c = 2.6\,\text{cm} \times L_c = 9.9\,\text{cm}$) were used with a configuration of two columns per section; feed concentration of 5 g/L of each enantiomer. In a first study,[19] an extract purity of 90.0% and raffinate purity of 91.6% were obtained, with a solvent consumption of 0.40 L of solvent per g of racemic mixture treated. Later,[20] for the same system, SMB operation led to a separation with 99.6% extract purity, 97.5% raffinate purity, and a solvent consumption of 1.34 L/g.

Influence of Mass Transfer Resistances on $\gamma_3 \times \gamma_2$ Separation Region

The conditions for a complete separation of a binary mixture can be defined in terms of the γ_j model parameters, which are directly related with the TMB operating variables (fluid and solid velocities in the four sections of the TMB unit). From the constraints presented in Eq. (2), those related to Sections 2 and 3 play the crucial role on the separation performance of the TMB, since is in these central zones that the separation between the two species takes place. The role of the adjacent Sections (1 and 4) is to prevent cross contamination and to allow the improvement of the continuous operation of the system by regenerating the solid and liquid phases. Nevertheless, the choice of γ_1 and γ_4 values is also important since it is directly related to solvent consumption. Taking into account these considerations, a region of complete separation in a $\gamma_3 \times \gamma_2$ plane can be defined. Considering that the constraints concerning Sections 1 and 4 are fulfilled, the $\gamma_3 \times \gamma_2$ plot is an important tool in the choice of best operating conditions.

If mass transfer resistance is important, we may not obtain a region for complete separation (100% pure enantiomers). In these cases, a purity criteria can be proposed and the region of separation (where both enantiomers purities are at least equal to the proposed purity criteria) can be evaluated using the steady-state TMB model described before.

The study of the influence of mass transfer resistance in the separation region was carried out keeping constant the internal liquid flow rates in Section 1 and 4 and also the solid flow rate, i.e., the ratio between fluid and solid interstitial velocities is fixed for Sections 1 and 4. Table 4 presents the operating conditions and model parameters used in the evaluation of the separation regions. Under these conditions, the eluent flow rate is constant and equal to $Q_E = (\gamma_1 - \gamma_4)\varepsilon V_c/t^* = 25.03\,\text{mL/min}$. It should be pointed out that the values used for γ_1 and γ_4 are both far away from the critical values stated

MARCEL DEKKER, INC.
270 Madison Avenue, New York, New York 10016

Table 4. Operating conditions and model parameters for the $\gamma_3 - \gamma_2$ plane.

SMB	Equivalent TMB
Column diameter: $D_c = 2.6\,\text{cm}$ Column length: $L_c = 9.9\,\text{cm}$ Configuration: 2 columns per section Bed porosity: $\varepsilon = 0.4$	Section length: $L_j = 2L_c = 19.8\,\text{cm}$
Peclet number: $Pe = 1000$	Peclet number: $Pe_j = 2Pe = 2000$
Feed concentration: $C_A = C_B = 5\,\text{g/L}$	
Switch time interval (min): $t^* = 3.3$	Solid flow rate (mL/min): $Q_s = (1 - \varepsilon)V_c/t^* = 9.56$
Flow rate in Section 1 (mL/min): $Q_1^* = 42.83$	Flow rate in Section 1 (mL/min): $Q_1 = Q_1^* - Q_S\,\varepsilon/(1 - \varepsilon) = 36.46$; $\gamma_1 = 5.722$
Flow rate in Section 4 (mL/min): $Q_4^* = 17.79$	Flow rate in Section 4 (mL/min): $Q_4 = Q_4^* - Q_S\,\varepsilon/(1 - \varepsilon) = 11.42$; $\gamma_4 = 1.793$

by the equilibrium theory. For Section 1, and considering mass transfer resistances negligible:

$$\gamma_1 > \gamma_1^{\min} = \frac{(1-\varepsilon)}{\varepsilon}(m + Qb_B) = \frac{(1-0.4)}{0.4}(1.35 + 7.32 \times 0.163) = 3.815 \tag{19}$$

In Section 4, the maximum value for γ_4 depends of the values of the flow-rate ratios γ_2 and γ_3. Nevertheless, the minor value for $\gamma_4^{\max}$ occurs for the vertex of the separation region in the $\gamma_3 \times \gamma_2$ plane, which corresponds to the better operating conditions since both solvent consumption and adsorbent productivity are optimized. Considering the equilibrium theory and for the operating conditions presented in Table 4, the vertex (point w in Fig. 2) is characterized by $\gamma_2 = 2.745$ and $\gamma_3 = 2.997$, which leads to

$$\gamma_4 < \gamma_4^{\max} = 2.714 \tag{20}$$

Figure 2 shows the separation regions obtained by simulation for different values of the mass-transfer coefficient using a 99% purity criteria. Inside each region both the raffinate and the extract are at least 99% pure. Also shown is the complete separation region (100% pure extract and raffinate) considering

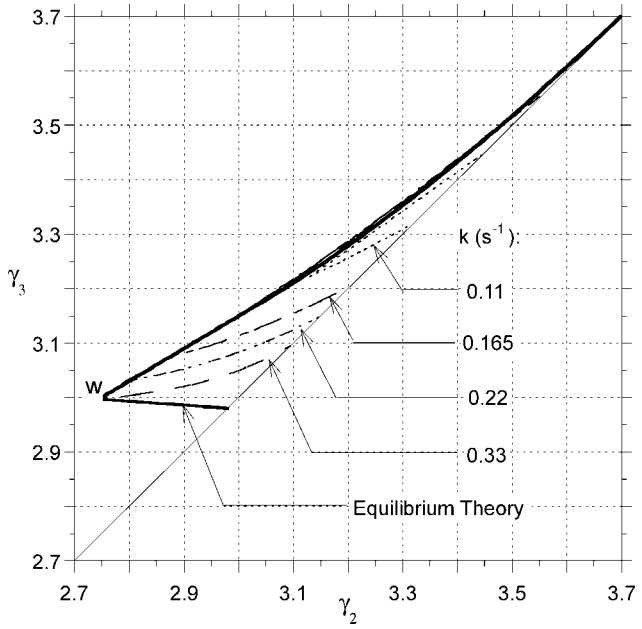

Figure 2. Influence of mass transfer resistance on the separation region (99% purity criteria). Also shown is the separation region considering equilibrium theory (100%). Operating conditions as in Table 4.

that mass transfer resistance is negligible (equilibrium theory). It can be concluded that mass transfer resistance can reduce significantly the region of separation of both enantiomers and that the region obtained for a lower mass-transfer coefficient lies inside the region obtained when mass transfer resistance is not so important. For mass-transfer coefficients lower than $0.11\,s^{-1}$, there is no 99% separation region. Although there are some differences between the two separation regions, the vertex point obtained considering the equilibrium theory is reached for $k = 0.33\,s^{-1}$.

Looking for the vertex points of the different separation regions presented in Fig. 2, we conclude that the mass transfer resistance also influences the better SMB operating conditions. Briefly, the lower the mass-transfer coefficient, the lower the maximum feed flow rate allowed in the SMB operation to obtain a desired enantiomers purity. Figure 3 shows the ratios between the real productivity [Fig. 3(a)] and solvent consumption [Fig. 3(b)] considering mass transfer resistance and the one obtained considering the equilibrium theory. According to Table 3, a productivity parameter is defined for each species, and corresponds to the amount of component (*A* or *B*)

Marcel Dekker, Inc.
270 Madison Avenue, New York, New York 10016

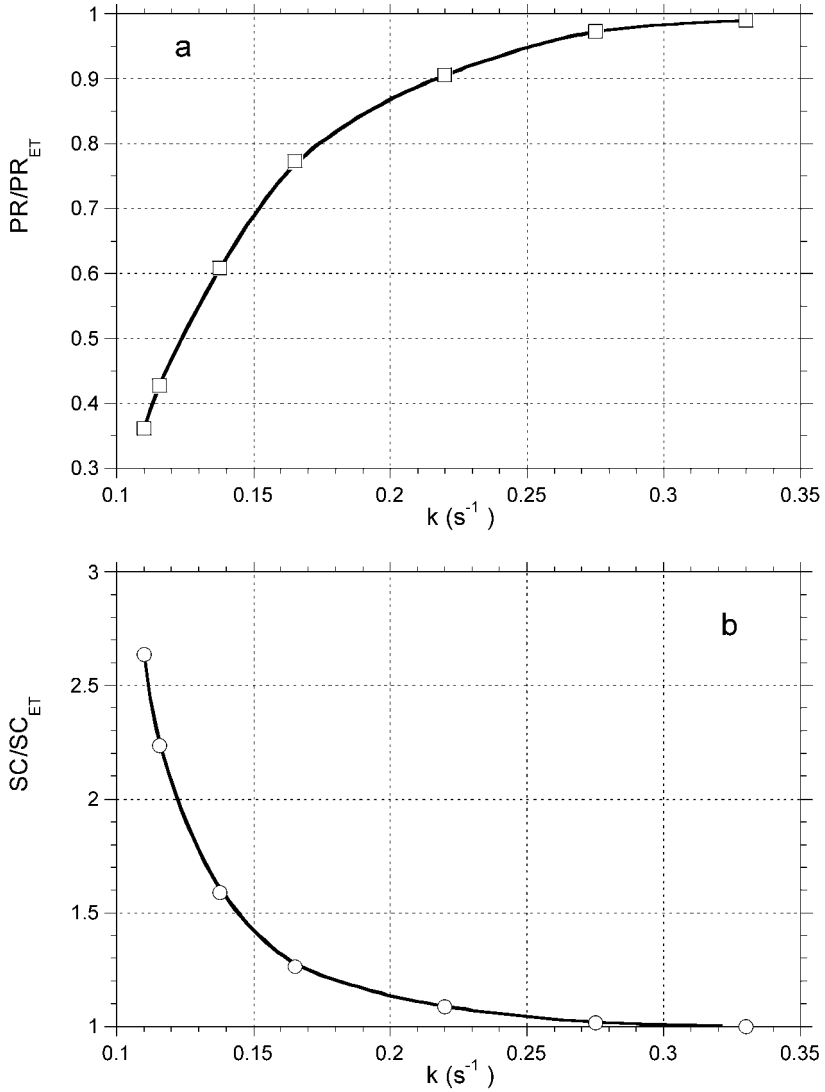

Figure 3. Influence of mass transfer resistance on the better SMB operating conditions (vertex points). (a) Ratio between the real productivity considering mass transfer resistance and the one obtained considering equilibrium theory; and (b) ratio between the real solvent consumption considering mass transfer resistance and the one obtained considering equilibrium theory. Operating conditions as in Table 4.

produced in the outlet stream (raffinate or extract, respectively), divided by the total volume of adsorbent used. However, for the case of equal extract and raffinate purities and $C_A^F = C_B^F$, the productivities of both species are also equal. For the purity criteria of 99%, the vertex point of a separation region leads to a productivity characterized by

$$PR = PR_A = PR_B = \frac{Q_R C_A^R}{V_{bed}} = \frac{Q_X C_B^X}{V_{bed}} = 0.99\frac{Q_F C_A^F}{V_{bed}} = 0.99\frac{Q_F C_B^F}{V_{bed}} \tag{21}$$

From Fig. 3, we can conclude that the better SMB operating conditions only approaches the ones derived by equilibrium theory for mass-transfer coefficients greater than $0.3\,s^{-1}$.

Influence of Mass Transfer Resistances on γ_1 and γ_4

It is interesting to study the importance of the choice of the flow-rate ratios in Sections 1 and 4, since it affects directly the value of solvent consumption:

$$SC = \frac{Q_E + Q_F}{Q_F(C_A^F + C_B^F)} = \frac{1}{C_A^F + C_B^F}\left[1 + \frac{\gamma_1 - \gamma_4}{\gamma_3 - \gamma_2}\right] \tag{22}$$

According to the equilibrium theory, the $\gamma_3 \times \gamma_2$ separation region will be constant providing that the values for γ_1 and γ_4 fulfill the restrictions of γ_1^{min} and γ_4^{max}, respectively [see Table 1; Eqs. (19) and (20)]. For the system under study, the minimum value for solvent consumption arises for the critical values γ_1^{min} and γ_4^{max}, and at the vertex point, i.e., $\gamma_1 = \gamma_1^{min} = 3.815$, $\gamma_2 = 2.745$, $\gamma_3 = 2.997$, and $\gamma_4 = \gamma_4^{max} = 2.714$. Considering that the feed concentrations are $C_A^F = C_B^F = 5\,g/L$, the minimum value for the solvent consumption expected for a 100% pure extract and raffinate, following equilibrium theory, is $SC = 0.537\,L/g$. However, these operating conditions are not followed in practice, since it corresponds to a situation where system robustness is very low. In the previous analysis of the influence of mass transfer resistances on the $\gamma_3 \times \gamma_2$ separation region, $\gamma_1 = 5.722$ and $\gamma_4 = 1.793$, was used both far away from the critical values stated by equilibrium theory. In this case, the vertex point stated by equilibrium theory ($\gamma_2 = 2.745$ and $\gamma_3 = 2.997$) will lead to a solvent consumption of $SC = 1.659\,L/g$, which is three times higher than the one obtained under critical operating conditions. This example shows how the choice of γ_1 and γ_4 is also important in SMB operation, and how the vertex point of the $\gamma_3 \times \gamma_2$

MARCEL DEKKER, INC.
270 Madison Avenue, New York, New York 10016

plot can hide completely different situations in terms of process solvent consumption.

It is our goal to study how mass transfer resistances can affect the choice of γ_1 and γ_4 and to compare it to the constraints concerning Sections 1 and 4 stated by equilibrium theory. First, we studied the influence of the γ_1 ratio on the separation regions considering the previous value of $\gamma_4 = 1.793$ and $k = 0.11\ s^{-1}$. The 99% separation region only occurs at $\gamma_1 = 4.158$, which is greater than the critical value stated by the equilibrium theory ($\gamma_1 = 3.815$). Also, the 99% separation region only reaches a constant size for a γ_1 greater than 6.5. Between those values ($4.158 < \gamma_1 < 6.5$), there is a kind of transition region in which the separation regions have varying size, as it was already noticed by Azevedo and Rodrigues for linear systems.[22] Figure 4 presents the three-dimensional plot and the two-dimensional projection on the $\gamma_3 \times \gamma_2$ plane resulting from the evaluation of the 99% separation regions for various values of γ_1. The separation volume is the region in the three-dimensional plot inside the boundaries of the white regions when γ_1 is continuously changed.

A similar procedure was followed to study the influence of the γ_4 ratio on the separation regions. Figure 5 presents the $\gamma_4 \times \gamma_2 \times \gamma_3$ three-dimensional plot and the two-dimensional projection on the $\gamma_3 \times \gamma_2$ plane resulting from the evaluation of the 99% separation regions for various values of γ_4, using a constant value of $\gamma_1 = 5.722$ and $k = 0.11\ s^{-1}$. We conclude that the effect of mass transfer resistance on the critical value for γ_4 is not so high as it is for γ_1. Because the critical value for γ_4 is not constant but depends on γ_2 and γ_3, a 99% separation region can be obtained even for γ_4 greater than 2.714. For values of $\gamma_4 < 2.5$ the separation regions reaches a constant size.

From the interpretation of the results obtained in Figs. 4 and 5 we conclude that, under mass transfer resistances, the $\gamma_3 \times \gamma_2$ separation region is no longer constant, but depends particularly of the γ_1 value. Also, the γ_1 critical value for which there is a separation region is higher than the one stated by equilibrium theory and depends not only on the equilibrium data, but also on mass transfer kinetics. We may conclude that, for a complete description of the operating conditions for SMB operation under nonideal conditions, it is necessary to evaluate a $\gamma_1 \times \gamma_2 \times \gamma_3$ separation volume instead of a more simple $\gamma_3 \times \gamma_2$ separation area. To conclude our study, it is interesting to analyze the evolution of the vertex points of the $\gamma_3 \times \gamma_2$ separation regions obtained under nonideal conditions as a function of γ_1 and its consequences on the SMB performance parameters. Figure 6 shows the results obtained. Due to mass transfer resistances, the 99% separation region only occurs for γ_1 higher than 4.158, instead of $\gamma_1^{min} = 3.815$, stated by the equilibrium theory. Due to the evolution of the $\gamma_3 \times \gamma_2$ separation regions presented in Fig. 4, for values of $\gamma_1 > 4.158$, the difference $(\gamma_3 - \gamma_2)$ will

MARCEL DEKKER, INC.
270 Madison Avenue, New York, New York 10016

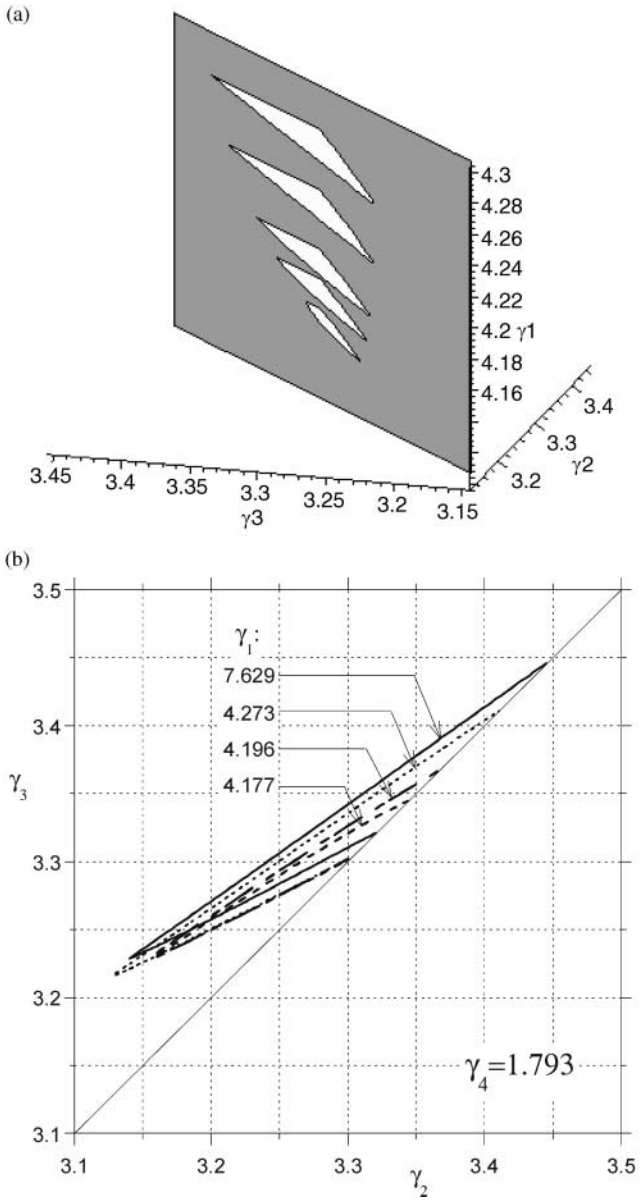

Figure 4. (a) Separation volume for 99% purity in a $\gamma_1 \times \gamma_2 \times \gamma_3$ 3-D coordinate system for $\gamma_4 = 1.793$ and $k = 0.11\,s^{-1}$; and (b) 2-D projection on the $\gamma_3 \times \gamma_2$ plane.

MARCEL DEKKER, INC.
270 Madison Avenue, New York, New York 10016

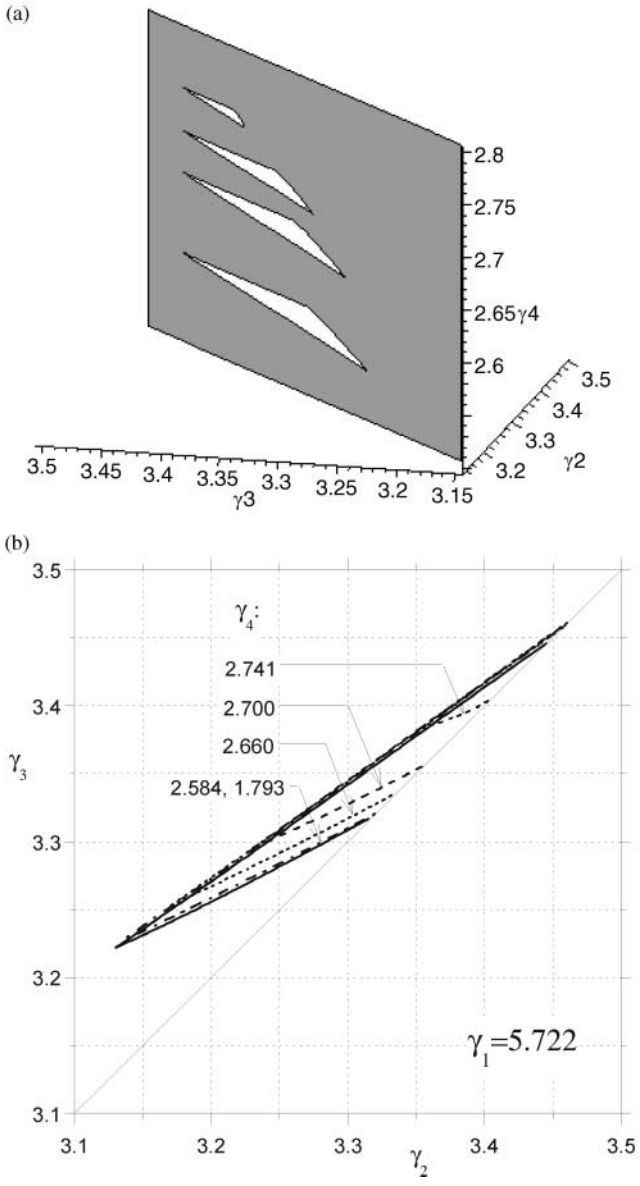

Figure 5. (a) Separation volume for 99% purity in a $\gamma_4 \times \gamma_2 \times \gamma_3$ 3-D coordinate system for $\gamma_1 = 5.722$ and $k = 0.11\ s^{-1}$; and (b) 2-D projection on the $\gamma_3 \times \gamma_2$ plane.

MARCEL DEKKER, INC.
270 Madison Avenue, New York, New York 10016

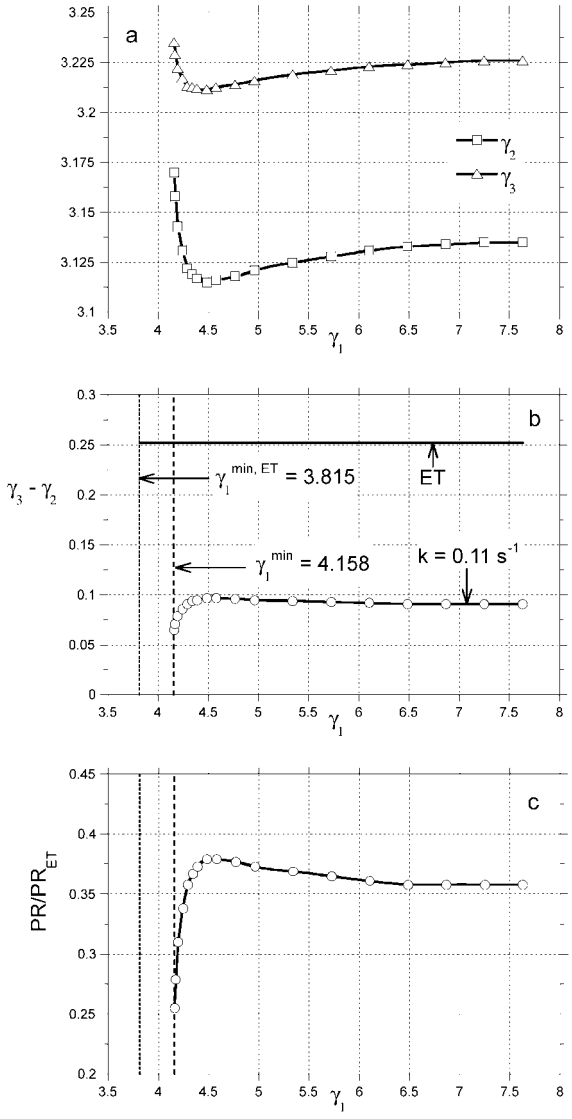

Figure 6. Influence of the flow-rate ratio in section 1, γ_1, under nonideal conditions ($k = 0.11\ s^{-1}$), on the vertex point of the $\gamma_3 \times \gamma_2$ separation region: (a) γ_3 and γ_2 at the vertex points; (b) $\gamma_3 - \gamma_2$ at the vertex points (also shown is the value obtained considering equilibrium theory); and (c) the ratio between the real productivity considering mass transfer resistance (at the vertex points) and the one obtained considering equilibrium theory.

MARCEL DEKKER, INC.
270 Madison Avenue, New York, New York 10016

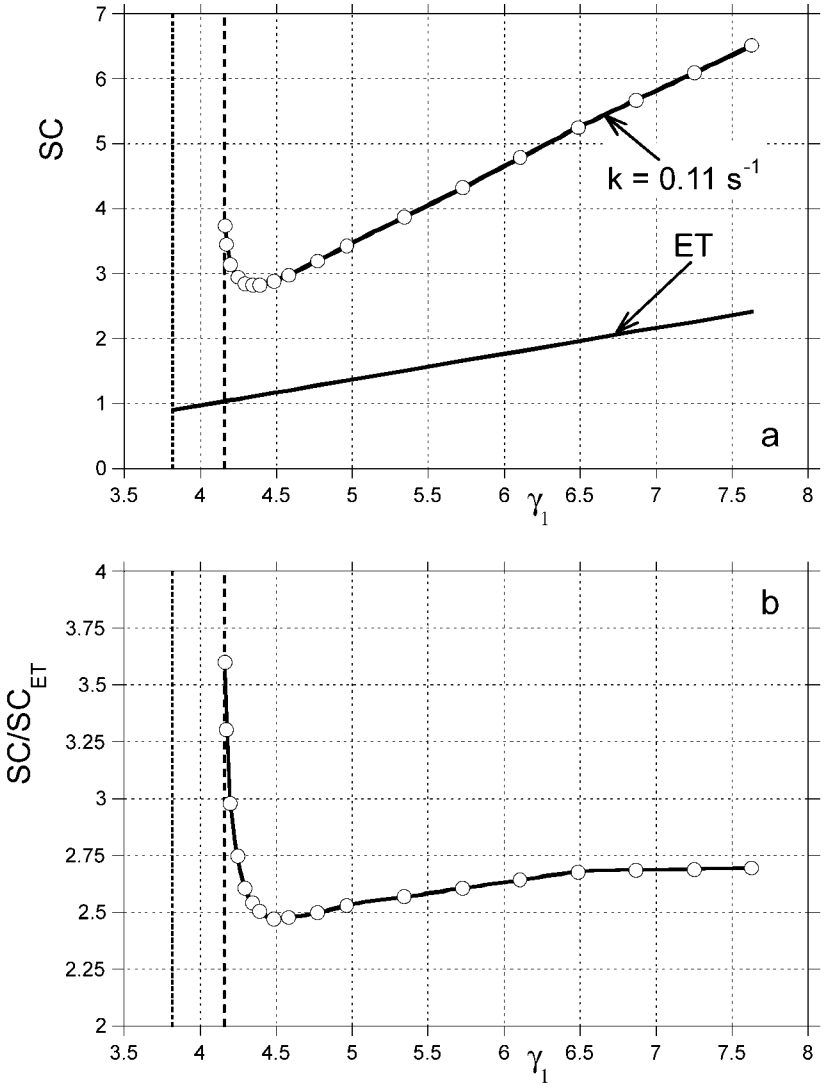

Figure 7. Influence of the flow-rate ratio in section 1, γ_1, under nonideal conditions ($k = 0.11\,s^{-1}$), on the vertex point of the $\gamma_3 \times \gamma_2$ separation region. (a) Solvent consumption (also shown is solvent consumption considering equilibrium theory); and (b) the ratio between the real solvent consumption considering mass transfer resistance (at the vertex points) and the one obtained considering equilibrium theory.

Marcel Dekker, Inc.
270 Madison Avenue, New York, New York 10016

increase until it reaches a constant value [see Fig. 6(b)]. This will influence the system productivity since this parameter is proportional to the feed flow rate and to the ($\gamma_3 - \gamma_2$) difference [see Fig. 6(c)]. Figure 7 presents the comparison in terms of solvent consumption. The typical linear dependence of solvent consumption on the γ_1 value found in equilibrium theory is not obtained under nonideal conditions. The optimum value of γ_1 in this situation is not only higher than the critical value stated by equilibrium theory ($\gamma_1 = 3.815$) but also higher than the lower γ_1 that allows a 99% separation region ($\gamma_1 = 4.158$). For the system in study, the optimum value will be $\gamma_1 = 4.5$.

CONCLUSION

The presence of mass transfer resistances can affect significantly the performance of the SMB operation, reducing the size of the separation region and modifying the better SMB operating conditions. Moreover, when mass transfer resistance is neglected, equilibrium theory states that the critical flow rate ratios required to achieve enantiomers separation depend exclusively on the equilibrium data. However, in the presence of mass transfer resistances, those critical values are more restrictive and should be evaluated through simulation.

This work shows how mass transfer resistances affect the constraint of Section 1. Particularly, the typical linear dependence of solvent consumption on the γ_1 ratio found in equilibrium theory is not obtained under nonideal conditions. In this case, simulation results show clearly that the optimum flow rate ratio in Section 1 is not only higher than the critical value stated by equilibrium theory, but also higher than the lower γ_1 value that allows a 99% separation region. Under nonideal conditions, numerical simulation is necessary to find a three-dimensional separation volume, instead of a two-dimensional separation area.

NOTATION

b = Adsorption isotherm parameter, $L_{fluid/g}$.
C = Fluid phase concentration, g/L.
D_L = Axial dispersion coefficient, cm^2/s.
D_c = Diameter of a SMB column, cm.
k = Mass-transfer coefficient, s^{-1}.
L_c = Length of a SMB column, cm.
L_j = Length of a TMB section, cm.

MARCEL DEKKER, INC.
270 Madison Avenue, New York, New York 10016

m = Adsorption isotherm parameter, $L_{fluid}/L_{particle}$.
m = Flow-rate ratio (Table 1).
Pe = Peclet number.
Q = Adsorption isotherm parameter, $g/L_{particle}$.
Q = Volumetric liquid flow rate in the TMB, cm^3/min.
Q^* = Volumetric liquid flow rate in the SMB, cm^3/min.
Q_s = Solid flow rate, cm^3_{solid}/min.
q = Average adsorbed phase concentration, $g/L_{particle}$.
q^* = Adsorbed phase concentration in equilibrium with C, $g/L_{particle}$.
t^* = Switch time interval, s.
u_s = Interstitial solid velocity in the TMB operation, cm/s.
V_c = Volume of a SMB column, cm^3.
v = Interstitial fluid velocity in the TMB operation, cm/s.
x = Dimensionless axial coordinate.

Greek Symbols

α = Number of mass transfer units.
γ = Ratio between fluid and solid interstitial velocities in the TMB operation.
ε = Bed porosity.
λ = Adsorption isotherm parameter, $\lambda = Q_b$.
ω = Roots of the quadratic Eq. (10).

Subscripts

A = Less retained component.
B = More retained component.
E = Eluent.
F = Feed.
i = Component index ($i = A, B$).
j = Section index ($j = 1, 2, 3, 4$).

REFERENCES

1. Anon. FDA's policy statement for the development of new stereoisomeric drugs. Chirality **1992**, *4*, 338.
2. Rekoske, J.E. Chiral separations. AIChE J. **2001**, *47*, 2.
3. Stinson, S.C. Chiral drugs. C&EN **1995**, *October 9*, 44.
4. Broughton, D.B.; Gerhold, C.G. Continuous Sorption Process Employing Fixed Bed of Sorbent and Moving Inlets and Outlets. U.S. Patent No. 2,985,589, 1961.

Marcel Dekker, Inc.
270 Madison Avenue, New York, New York 10016

5. Nicoud, R.M. The separation of optical isomers by simulated moving bed chromatography. Pharm. Tech. Europe **1999**, *11* (3), 36.
6. Nicoud, R.M. The separation of optical isomers by simulated moving bed chromatography. Pharm. Tech. Europe **1999**, *11* (4), 28.
7. McCoy, M. SMB emerges as chiral technique. C&EN **2000**, *June 19*, 17.
8. Cox, G.B. Preparative enantioselective chromatography. In *Current Status and Future Trends*; PREPTECH—Preparative and Process Scale Technology in the Manufacturing of Chemicals and Pharmaceuticals: Mainz, Germany, April 18–20, 2001.
9. Stinson, S.C. Chiral chemistry. C&EN **2001**, *May 14*, 45.
10. Nicoud, R.M. The simulated moving bed: a powerful chromatographic process. LC-GC Int. **1992**, *5*, 43.
11. Gattuso, M.J.; McCulloch, B.; House, D.W.; Baumann, W.M.; Gottschall, K. Simulated moving bed technology—the preparation of single enantiomer drugs. Pharm. Tech. Europe **1996**, *8*, 20.
12. Nicoud, R.M.; Majors, R.E. Simulated moving bed chromatography for preparative separations. LC-GC Europe **2000**, *13*, 887.
13. Blehaut, J.; Hauck, W.; Nicoud, R.M. Simulated moving bed (S.M.B.): principle and application to chiral separations. Seminar on Batch and SMB Design and Applications. AIChE Meeting, Chicago, March 2001.
14. Broughton, D.B. Production-scale adsorptive separations of liquid mixtures by simulated moving-bed technology. Sep. Sci. Technol. **1984**, *19*, 723.
15. Ruthven, D.M.; Ching, C.B. Counter-current and simulated counter-current adsorption separation processes. Chem. Engng Sci. **1989**, *44*, 1011.
16. Pais, L.S.; Loureiro, J.M.; Rodrigues, A.E. Separation of 1,1′-bi-2-naphthol enantiomers by continuous chromatography in simulated moving bed. Chem. Engng Sci. **1997**, *52*, 245.
17. Pais, L.S.; Loureiro, J.M.; Rodrigues, A.E. Modeling, strategies for enantiomers separation by SMB chromatography. AIChE J. **1998**, *44*, 561.
18. Pais, L.S.; Loureiro, J.M.; Rodrigues, A.E. Modeling separation and operation of a simulated moving bed for continuous chromatographic separation of 1,1′-bi-2-naphthol enantiomers. J. Chromatogr. A **1997**, *769*, 25.
19. Pais, L.S.; Loureiro, J.M.; Rodrigues, A.E. Separation of enantiomers of a chiral epoxide by simulated moving bed chromatography. J. Chromatogr. A **1998**, *827*, 215.
20. Pais, L.S.; Loureiro, J.M.; Rodrigues, A.E. Chiral separation by SMB chromatography. Sep. Purif. Technol. **2000**, *20*, 67.

MARCEL DEKKER, INC.
270 Madison Avenue, New York, New York 10016

21. Azevedo, D.C.S.; Pais, L.S.; Rodrigues, A.E. Enantiomers separation by simulated moving bed chromatography. Non-instantaneous equilibrium at the solid-fluid interface. J. Chromatogr. A **1999**, *865*, 187.
22. Azevedo, D.C.S.; Rodrigues, A.E. Design of a simulated moving bed in the presence of mass-transfer resistances. AIChE J. **1999**, *45*, 956.
23. Azevedo, D.C.S.; Rodrigues, A.E. Bilinear driving force approximation in the modeling of a simulated moving bed using bidisperse adsorbents. Ind. Eng. Chem. Res. **1999**, *38*, 3519.
24. Azevedo, D.C.S.; Rodrigues, A.E. Obtainment of high-fructose solutions from cashew (*Anacardium occidentale*) apple juice by simulated moving-bed chromatography. Sep. Sci. Technol. **2000**, *35*, 2561.
25. Rodrigues, A.E.; Pais, L.S. Modelling and simulation in SMB for chiral purification. In *Chiral Separation Techniques. A Practical Approach—Second Completely Revised and Update Edition*; Subramanian, G., Ed.; Wiley-VCH; 2000; 221.
26. Mazzotti, M.; Storti, G.; Morbidelli, M. Optimal operation of simulated moving bed units for nonlinear chromatographic separations. J. Chromatogr. A **1997**, *769*, 3.
27. Ma, Z.; Wang, N. Standing wave analysis of SMB chromatography: linear systems. AIChE J. **1997**, *43*, 2488.
28. Zhong, G.; Guiochon, G. Simulated moving bed chromatography. Effects of axial dispersion and mass transfer under linear conditions. Chem. Engng Sci. **1997**, *52*, 3117.
29. Yun, T.; Bensetiti, Z.; Zhong, G.; Guiochon, G. Effect of column efficiency on the internal concentration profiles and the performance of a simulated moving-bed unit in the case of a linear isotherm. J. Chromatogr. A **1997**, *758*, 175.
30. Xie, Y.; Wu, D.; Ma, Z.; Wang, N. Extended standing wave design method for simulated moving bed chromatography: linear systems. Ind. Eng. Chem. Res. **2000**, *39*, 1993.
31. Charton, F.; Nicoud, R.M. Complete design of a simulated moving bed. J. Chromatogr. A **1995**, *702*, 97.
32. Strube, J.; Altenhoner, U.; Meurer, M.; Schmidt-Traub, H.; Schulte, M. Dynamic simulation of simulated moving-bed chromatographic processes for the optimization of chiral separations. J. Chromatogr. A **1997**, *769*, 81.
33. Mallmann, T.; Burris, B.D.; Ma, Z.; Wang, N. Standing wave design of nonlinear SMB systems for fructose purification. AIChE J. **1998**, *44*, 2628.
34. Wu, D.J.; Xie, Y.; Ma, Z.; Wang, N. Design of simulated moving bed chromatography for amino acid separations. Ind. Eng. Chem. Res. **1998**, *37*, 4023.

MARCEL DEKKER, INC.
270 Madison Avenue, New York, New York 10016

35. Migliorini, C.; Gentilini, A.; Mazzotti, M.; Morbidelli, M. Design of simulated moving bed units under nonideal conditions. Ind. Eng. Chem. Res. **1999**, *38*, 2400.
36. Biressi, G.; Ludemann-Hombourger, O.; Mazzotti, M.; Nicoud, R.M.; Morbidelli, M. Design and optimisation of a simulated moving bed unit: role of deviations from equilibrium theory. J. Chromatogr. A **2000**, *876*, 3.
37. Ludemann-Hombourger, O.; Nicoud, R.M.; Bailly, M. The varicol process: a new multicolumn continuous chromatographic process. Sep. Sci. Technol. **2000**, *35*, 1829.
38. Bader, G.; Ascher, U. A new basis implementation for a mixed order boundary value ODE solver. SIAM J. Sci. Stat. Comput. **1987**, *8*, 483.
39. Ascher, U.; Christiansen, J.; Russell, R.D. A collocation solver for mixed order systems of boundary value problems. Math. Comput. **1979**, *33*, 659.
40. Ascher, U.; Christiansen, J.; Russell, R.D. Collocation software for boundary-value ODEs. ACM Trans. Math. Software **1981**, *7*, 209.

Received November 2002
Revised July 2003